

Supporting Information

Multifunctional Nanocomposites for Targeted, Photothermal, and Chemotherapy

Ming Zhang,[†] Fan Wu,[†] Wentao Wang,[†] Jian Shen,[†] Ninglin Zhou,^{,†} Changzhu Wu^{*,‡}*

[†]Jiangsu Collaborative Innovation Center for Biological Functional Materials, Jiangsu Key Laboratory of Biofunctional Materials, College of Chemistry and Materials Science, Nanjing Normal University, Nanjing 210023, PR China

[‡]Danish Institute for Advanced Study (DIAS) and Department of Physics, Chemistry and Pharmacy, University of Southern Denmark, Odense 5230, Denmark

EXPERIMENTAL SECTION

Synthesis of AuNPs and ZnO-capped Au NPs. The synthetic procedure was the same as the previously reported method by Klug and co-workers [1], as shown in Figure S1A.

Synthesis of PEG-functionalized GO. GO suspension was prepared from graphite powder according to the previously reported literature [2]. GO solution was obtained by the filtration of GO suspension through ultrasonication (40 kHz, 150 watts) for 1 h. The obtained GO was then dispersed into deionized (DI) water for further use. For the synthesis of PEG-GO, 10 mL GO solution (3 mg/mL) was dispersed in NaOH solution (0.12 g/mL), and then sonicated for 4 h. The neutralized GO was immediately subjected to the centrifugation, and the obtained GO was washed several times with DI water. The GO solution (1 mg/mL) was then added into the COOH-PEG-NH₂ solution (3 mg/mL). The solution was sonicated for 5 min. After

that, EDC was added to the mixture under magnetic stirring at 37 °C for 24 h. Finally, the as-prepared PEG-GO washed several times with DI water to remove unreacted COOH-PEG-NH₂.

PEG-GO embellished with Au-His@a-ZnO NPs. For the further conjugation, PEG-GO (10 mg) and Au-His@a-ZnO NPs (100 mg) were dispersed in DI water (10 mL), then 5 mL EDC solution (10 mg/mL) was added, and stirred for 30 min. Then, 15 mL EDC solution was added again and stirred for 12 h. Subsequently, the mixture was purified and centrifugated (13,000 rpm, 2 h). After that, the supernatant was collected and filtered with 100 K ultrafilter. The obtained solids were repeatedly washed with the aqueous solution (10% NaCl, 10% urea) in the ultrafilter to remove unreacted Au-His@a-ZnO NPs, finally obtaining a stable solution (GO@Au-His@a-ZnO NCs).

Synthesis of the Anti-EGFR aptamer conjugated GO@Au-His@a-ZnO NPs. The anti-EGFR DNA aptamer (Apt) (5'-COOH-TGA ATG TTG TTT TTT CTC TTT TCT ATA GTA-3') and the scrambled control Apt (5'-COOH-AAA AAA AAA AAA ATG CCA CCT CGG TAG TCC TAA AGG GCA AAT TCG GAA CGC AGG TAC TTA C-3') were used in this work. Apt was covalently conjugated with Apt-GO@Au-His@a-ZnO NCs to target the surface of the cancer cells. This conjugation was achieved via amide coupling between -COOH groups of Apt and the -NH₂ groups of Apt-GO@Au-His@a-ZnO NCs using EDC/NHS. The process was operated as follows: 100 µL COOH-modified Apt (10 µM) was first incubated with EDC (10 mg) and NHS (8 mg). Then, the mixture was stirred for 3 h at 37 °C in darkness. Subsequently, 200 µL 1% Apt-GO@Au-His@a-ZnO NCs solution was added, and reaction was performed for 12 h. After that, the unreacted Apt was isolated through ultrafiltration and centrifugation. The purified Apt-GO@Au-His@a-ZnO NCs was diluted with 10 times with PBS (pH = 7.4) as the stock concentration.

Photothermal conversion of the GO@Au-His@a-ZnO NCs. To quantitatively determine the photothermal conversion of the GO@Au-His@a-ZnO NCs, the GO@Au-His@a-ZnO NCs were dispersed in DI water under NIR laser (808 nm, 0.5-1.5 W/cm²) irradiation for 5 min. During the course of irradiation, the temperature of the GO@Au-His@a-ZnO NCs solution was measured every 1 s through a thermocouple probe until reaching a steady-state temperature. The photothermal conversion efficiency (η) was calculated as follows:

$$\eta = \langle hA(T_{\max} - T_{\text{Surr}}) - Q_{\text{Dis}} \rangle / \langle I(1 - 10^{-A_{808}}) \rangle$$

where h represents the coefficient of heat transmission, T_{\max} and T_{Surr} represent the equilibrium and environmental temperature, A represents the superficial area of the container, Q_{Dis} is the thermal dissipation, A_{808} is the absorbance of GO@Au-His@a-ZnO NCs, and I is irradiation laser power. The value of hA could be got through the following formula :

$$\tau_s = (m_D \cdot C_D) / hA$$

The sample system time constant is represented by τ_s ; m_D is the solvent mass (1.0 g); C_D represents solvent heat capacity (4.2 J/g). To acquire τ_s , the other equation is used as following:

$$t = -\tau_s (\ln \theta)$$

Where θ could be got through the ratio of T and T_{\max} .

Hemolysis Assay. Red blood cells (RBCs) were obtained through centrifugation and suction (blood supported by Jiangsu Blood Centre). The RBCs was washed several times with PBS and then dilute to one-tenth of their original volume. Apt@GO@Au-His@a-ZnO NCs solution with different concentrations, 1.0 mL of PBS (negative control), and 1.0 mL of DI water (positive control), was incubated with

the diluted RBCs suspension in a homogeneous phase at 37 °C for 1 h. Afterward, the mixture was centrifugated (1,500 rpm, 10 min), and then the absorbance of the clear solution was measured at 545 nm. All tests were repeated three times to calculate the standard deviation.

***In vitro* blood coagulation.** The rats (200 ± 20 g) were divided into four groups randomly. The rats received the intravenous injection of Apt@GO@Au-His@a-ZnO NCs dispersion (in saline) *via* the tail vein. The sample doses for intravenous injection to each group were 0.1, 1, or 10 mg/kg, and saline was chosen as the control. After one day, the rats were anesthetized and then subjected for APTT and PT assays.

Morphological changes of RBCs. Blood was collected from rat's orbital sinus after intravenous (i.v.) injection of NCs. RBCs were separated by centrifugation (1,500 rpm, 10 min) of whole blood. The platelets and plasma were discarded. The supernatant was repeatedly washed with the stroke-physiological saline solution (SPSS) and then redispersed in SPSS. The pellet collected after centrifugation was dispersed in SPSS. Finally, the droplet containing RBCs was dropped on clean glass slides and pictured under the optical microscope.

DOX loading (Apt@GO@Au-His@a-ZnO@DOX NCs). The anticancer drug (DOX) solution (2.5 mL, 1.0 mg/mL) was added into the Apt@GO@Au-His@a-ZnO NCs solution, which was acted as the DOX carrier. The mixture was stirred for 24 h under darkness. The amount of loaded DOX in Apt@GO@Au-His@a-ZnO NCs was quantified according to the 490 nm absorbance of DOX. The DOX loading efficiency was determined with the following formula:

$$\text{Loading efficiency (\%)} = (\text{weight of DOX in NCs} / \text{weight of DOX added}) \times 100$$

DOX release of the Apt@GO@Au-His@a-ZnO@DOX NCs. Three dialysis bags (8-14 kD) containing Apt@GO@Au-His@a-ZnO@DOX NCs solution (1 mL) were placed into different environments (pH 5.5/7.4 and pH 5.5+NIR laser). Apt@GO@Au-His@a-ZnO@DOX NCs solution (50 μ L) from each sample solution was extracted at different time intervals. Another Apt@GO@Au-His@a-ZnO@DOX NCs (50 μ L) solution was extracted after NIR laser (808 nm, 1.5 W/cm²) irradiation at different time intervals. Finally, the amount of released DOX in Apt@GO@Au-His@a-ZnO@DOX NCs was quantified according to the 490 nm absorption of DOX.

Cell culture experiments. All cell lines originally purchased from the CSA were cultured under 5% CO₂ at 37 °C. All cells were cultured in DMEM media containing 1% streptomycin and 10% FBS.

Western blotting. Bradford Protein Assay Kit was used to determine the protein concentration of cell lysates among A549/H522, equal twenty-five micrograms of the whole protein were loaded on 10-15% SDDS-PAGE with 100 V for about 2-3 h, after which transferred to NC membrane with 350 mA for about 1.5 h. The membranes was incubated in blocking buffer contained TBST with 5% skims milk for 1 h at 37 °C. After that, membranes were immunoblotted with antibody for EGFR (prepared with 5% skims milk) at 4 °C for 12 h. Then the membranes were washed with TBST for three times (10 min/time). Lately, the membranes were exposed to HRP-conjugated second-antibody for 1 h at 37 °C and washed again. To this end, the membranes were observed with luminateTM Forte Western HRP substrate. The GAPDH protein level was tested and used as the internal control.

Interaction assay between Apt@GO@Au-His@a-ZnO@DOX NCs and A549

cells. A549 cells (10^5 cells/well) were cultured in DMEM containing 10% FBS at 37 °C under 5% CO₂ for 24 h. After adhesion, cells were washed several times with PBS and replaced with DMEM including Apt@GO@Au-His@a-ZnO@DOX and GO@Au-His@a-ZnO@DOX NCs at the same amount of DOX. The mixture was incubated for 1 h under 5% CO₂ at 37 °C. The cells were then washed several times with PBS and visualized under an LSCM.

***In vivo* imaging.** For NIR-induced intracellular DOX release study, A549 cells were treated with DOX and Apt-GO@Au-His@a-ZnO@DOX NCs containing the same amount of DOX for 1 h and then treated with or without NIR light (808 nm, 0.5 W/cm²) for 10 min. Cells were washed several times with PBS, and then observed and imaged using CLSM.

***In vitro* cytotoxicity of GO@Au-His@a-ZnO NCs and combination therapy of Apt@GO@Au-His@a-ZnO@DOX NCs.** Cells were cultured in the 96-well plates at 5×10^4 cells/well for 12 h. Then cells were incubated with DMEM including various concentrations of Apt@GO@Au-His@a-ZnO NCs for 24 h. Next, the standard MTT assay [3] was used to evaluate the cytotoxicities of GO@Au-His@a-ZnO NCs.

For *in vitro* combination therapy, A549 cells were incubated with Apt@GO@Au-His@a-ZnO@DOX NCs (L+), Apt@GO@Au-His@a-ZnO NCs, Apt@GO@Au-His@a-ZnO@DOX NCs, Apt@GO@Au-His@a-ZnO NCs (L+), DOX NCs (L+), and DOX for 4 h, and then the incubation was subjected to NIR laser irradiated (808 nm, 1.0 W/cm²) for 10 min. The dead and live cells were determined through co-staining of PI and calcein AM. Meanwhile, the standard MTT assay was performed to evaluate relative cell viabilities. The experimental steps were as follows: A549 cells were incubated with Apt@GO@Au-His@a-ZnO@DOX NCs (L+), Apt@GO@Au-His@a-ZnO@DOX NCs, Apt@GO@Au-His@a-ZnO NCs (L+),

DOX (L+), and DOX for 1 h, washed several times with DMEM and then exposed to NIR laser (808 nm, 0.5-1.5 W/cm²) for 5 min.

***In vivo* fluorescent and thermal imaging.** A549 tumor model with a tumor volume of 40-50 mm³ was used in this test. DOX, Au-His@a-ZnO@DOX NCs, and Apt@GO@Au-His@a-ZnO@GO@DOX NCs were injected into mice. After 24 h post-injection, living animal fluorescence microscopy imaging system was carried out for fluorescent imaging of mice. Then, the mice were sacrificed by exsanguinations, and the tumor and major organs were harvested. IR thermal camera was used to shoot thermographs of the tumors treated with NIR laser (808 nm, 1.5 W/cm²) for 5 min.

***In vivo* combination therapy.** A549 tumor-bearing mice were 6-7 weeks old with ≈ 100 mm³ tumor volume and divided into seven groups. PBS (50 μ L), Apt@GO@Au-His@a-ZnO NCs, Apt@GO@Au-His@a-ZnO NCs (L+), free DOX, DOX (L+), Apt@GO@Au-His@a-ZnO@DOX NCs, Apt@GO@Au-His@a-ZnO NCs (L+), and Apt@GO@Au-His@a-ZnO@DOX NCs (L+) were locally administered into tumors with 10 mg/kg mice body weight. After 15 min injecting, mice was irradiated with NIR laser (808 nm, 1.5 W/cm²) for 5 min. Tumor sizes were monitored by a digital caliper every 2 days and their volumes were calculated as the volume = width²/2 \times length. The body weights were regularly observed until mice were sacrificed. The main organs of the mice were removed after a variety of treatments. Organ index (in g/g) was calculated as wet weight (the individual organ) / weight (the whole body). H&E staining of organs and tumors were performed to obtain optical microscope pictures. The concentration of NCs in the main organs was measured by ICP-MS analysis. TUNEL apoptosis assay kit was used to measure the combination therapy. The blood sample was separated from the mice bodies to measure the blood biochemical index.

Statistical analysis. Data were exhibited as the mean value \pm standard deviation while significance was analyzed by the Student's t-test. Differences were recorded as significant for $P < 0.05$.

Supporting Figure.

Characteristics of the Au-His@a-ZnO NPs. A number of techniques were used to characterize the core-shell structure and formation. The XRD spectra (Figure S1B) displayed that the gold core has crystalline structure, which agrees with the literature [1]. Elemental analyses by XPS (Figure S1C) and EDS (Figure S1D) show that the core-shell NPs are composed of Au, Zn, and O (the EDS signals of Cu come from the TEM grid). In particular, XPS data shows that Au-His@a-ZnO has composition of C, O, N, Zn, and Au with 38.49 wt %, 23.66 wt %, 12.80 wt %, 9.56 wt %, and 15.49 wt %, respectively, revealing its gold and zinc dual-doped NPs. The lattice fringes in AuNPs core without crystallinity are observed by the high-resolution TEM (HRTEM) in Figure S1E, a, indicating the amorphous structure of the shell. STEM-EDS element maps (Figure S1E, b) disclose the presence of O and Zn element in the shell, where O 1s and Zn 2p_{3/2} are subsequently confirmed by high-resolution XPS, thus suggesting the ZnO formation in the shell. A close observation by HRTEM (Figure S1E, b) confirms the core-shell structure of Au-His@a-ZnO NPs. These characterizations prove the successful formation of core-shell-structured Au-His@a-ZnO NPs with a mean thicknesses of the shell domain of ~ 2.5 nm. The N element peak in XPS spectra (Figure S1C) shows that the His molecules cover on the surface of AuNPs shell, suggesting their presence and mediation function during the course of particle formation.

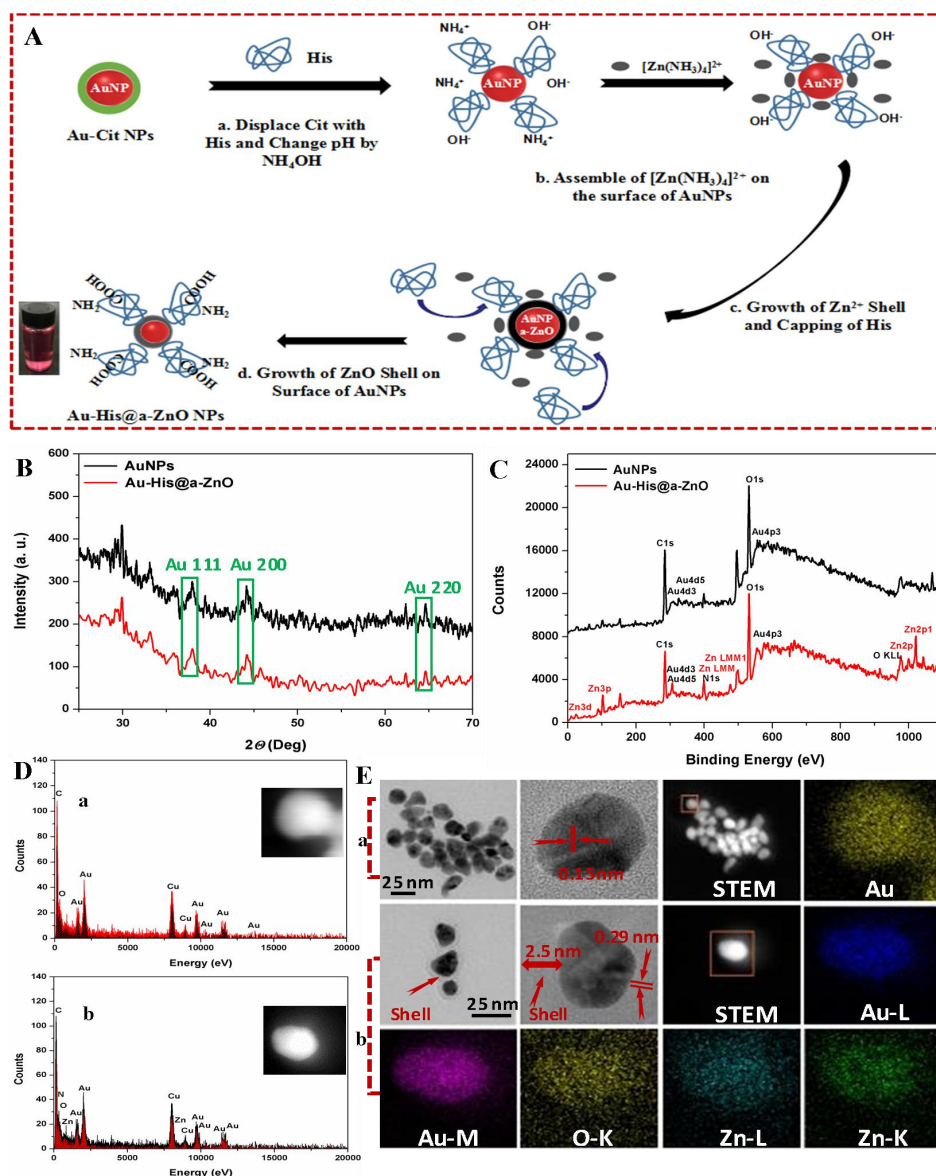


Figure S1. (A) A schematic illustration for the synthesis process of Au-His@a-ZnO NPs. (B) XRD spectra and (C) XPS survey scan of Au-His@a-ZnO NPs. (D) EDS characterization of (a) AuNPs and (b) Au-His@a-ZnO NPs. The inset is the dark-field TEM images. (E) TEM, HRTEM and elemental maps image of (a) AuNPs and (b) Au-His@a-ZnO NPs.

XPS of Au-His@a-ZnO NPs. Figure S2 shows the O 1s and Zn 2p_{3/2} spectra of the as-prepared Au-His@a-ZnO NPs. These results confirm that the shell materials of NPs are ZnO rather than Zn(OH)₂. The O 1s spectra present the main peak at 530.6 eV, which is due to the O²⁻ within the ZnO, and the Zn-O band at ~531.6 eV. A peak of adsorbed O species appears at 533.2 eV, which could attribute to H₂O or O₂, etc.

Moreover, the peak at 1021.2 eV attributed to ZnO was clearly observed, indicating the Zn^{2+} in the shell of NPs due to the formation of ZnO through His-mediation. This result is consistent with the reported paper for Au-His@a-ZnO NPs [1].

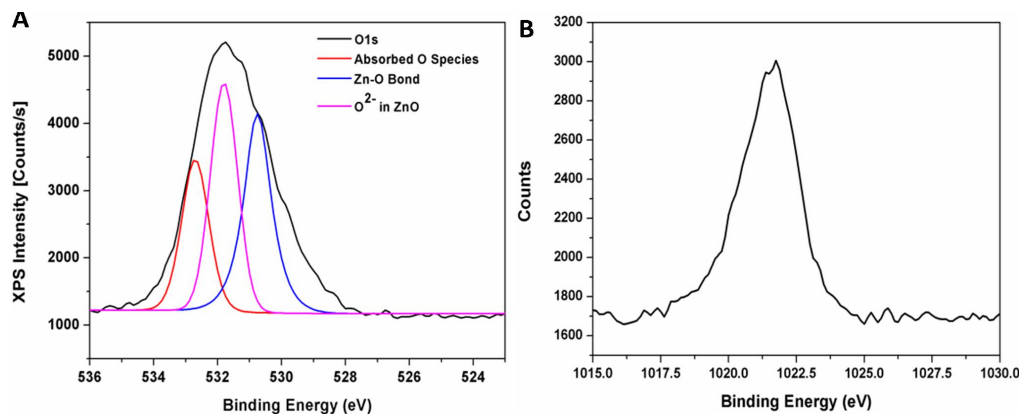


Figure S2. XPS scans of (A) O 1s and (B) Zn 2p_{3/2} spectra for Au-His@a-ZnO NPs.

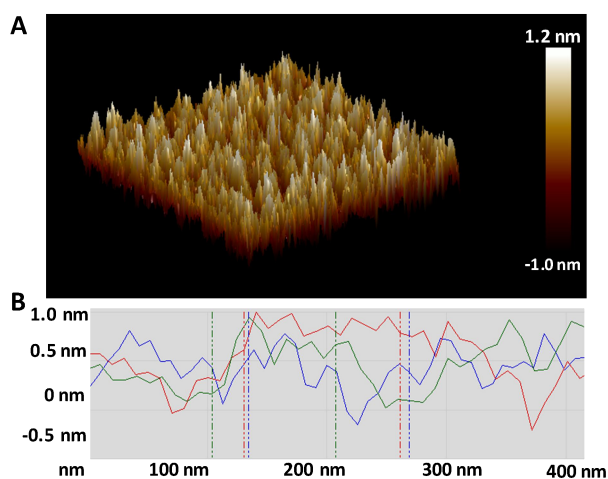


Figure S3. (A) AFM image of GO, and (B) the height profile of GO.

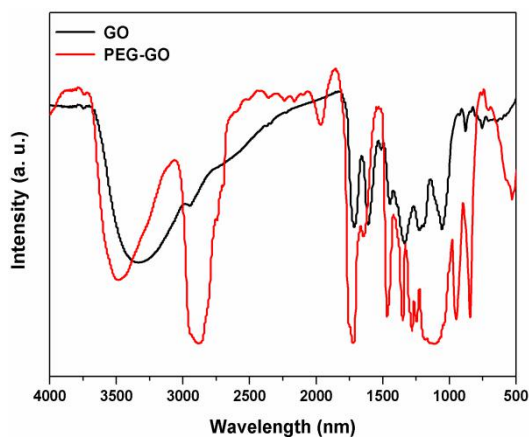


Figure S4. FT-IR spectra of PEG-GO and GO.

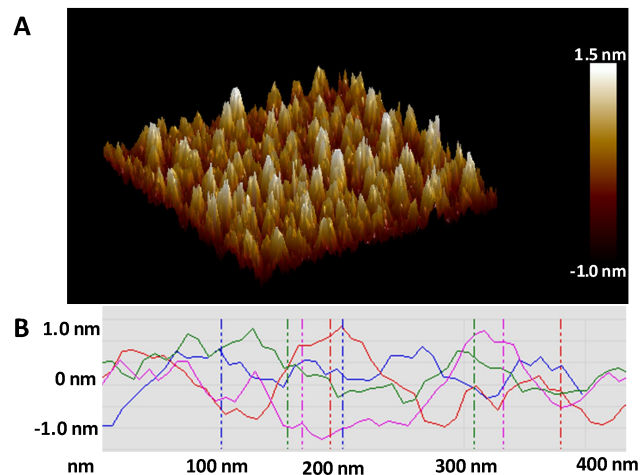


Figure S5. (A) AFM image of PEG-GO, and (B) the height profile of the PEG-GO.

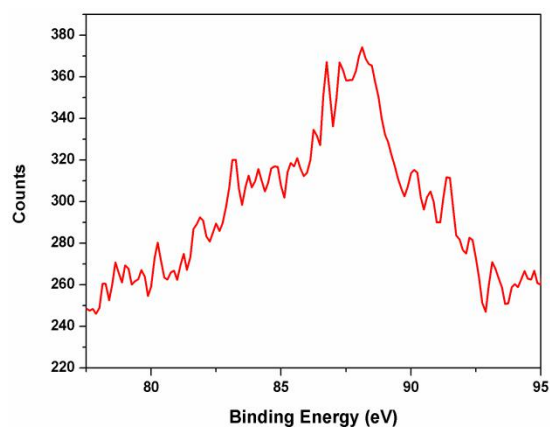


Figure S6. XPS scans of Au 4f spectra for Au-His@a-ZnO NPs.

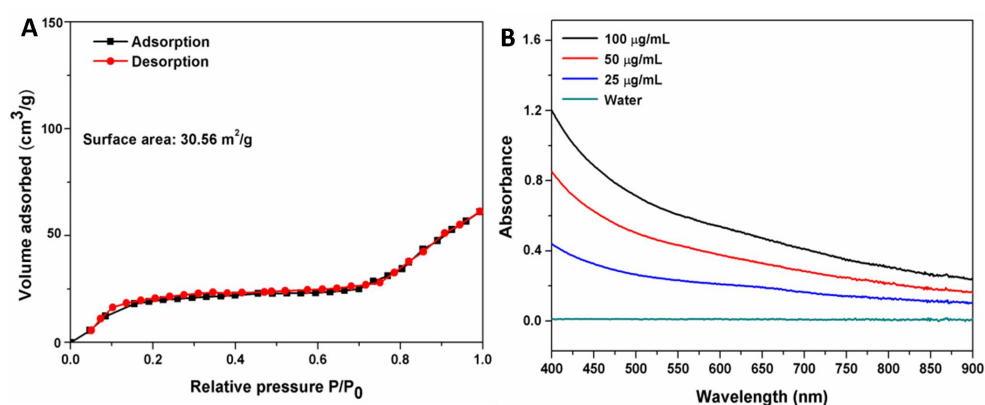


Figure S7. (A) Specific surface area analysis of GO@Au-His@a-ZnO NCs. (B) UV-vis-NIR spectra of GO@Au-His@a-ZnO NCs solutions with different concentrations.

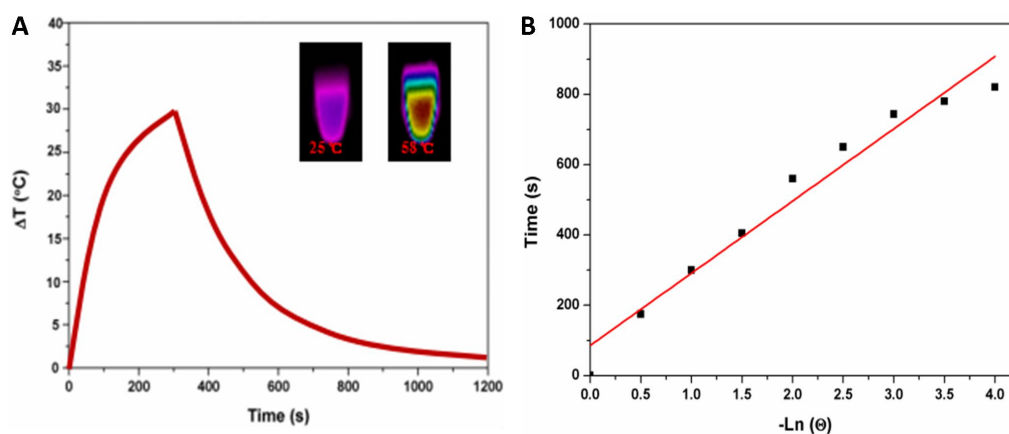


Figure S8. (A) Photothermal effect of GO@Au-His@a-ZnO NCs solution (50 $\mu\text{g/mL}$) under NIR laser irradiation. (B) The plot of cooling time and $-\ln\theta$ obtained from the cooling time.

Samples	Maximum Temperature ($^{\circ}\text{C}$)	Photothermal
		Conversion Efficiency (%)
GO nanosheets	63	41
Au-His@a-ZnONPs	51	29
GO@Au-His@a-ZnO NCs	58	38

Table S1. Comparisons of photothermal efficiency of GO nanosheets, Au-His@a-ZnO NPs, and GO@Au-His@a-ZnO NCs.

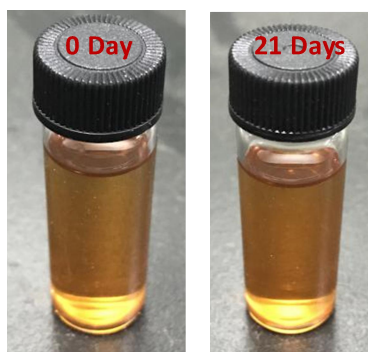


Figure S9. Photos of Apt@GO@Au-His@a-ZnO@DOX NCs in PBS after 21 days.

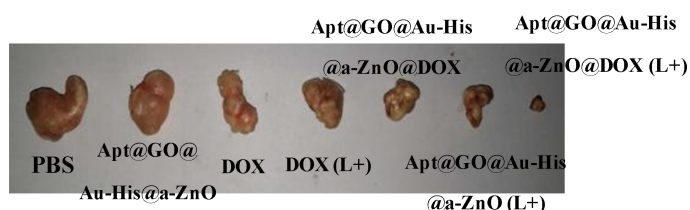


Figure S10. Photos of the excised tumors after various treatments.

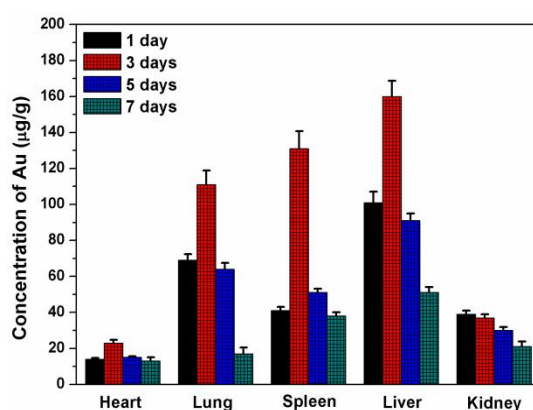


Figure S11. Biodistribution of Apt@GO@Au-His@a-ZnO NCs at various time after i.v injection of NCs (n=5).

Reference

- [1] Klug, M. T.; Dorval Courchesne, N. M.; Lee, Y. E.; Yun, D. S.; Qi, J.; Heldman, N. C.; Belcher, A. M. Mediated Growth of Zinc Chalcogen Shells on Gold Nanoparticles by Free-Base Amino Acids. *Chem. Mater.* **2017**, *29*, 6993-7001.
- [2] Wang, Y. H.; Wang, H. G.; Liu, D. P.; Song, S. Y.; Wang, X.; Zhang, H. J.; Graphene oxide covalently grafted upconversion nanoparticles for combined NIR mediated imaging and photothermal/photodynamic cancer therapy. *Biomaterials* **2013**, *34*, 7715-7724.
- [3] Zhang, M.; Chi, C.; Yuan, P.; Su, Y.; Shao, M.; Zhou, N. A Hydrothermal Route to Multicolor Luminescent Carbon Dots from Adenosine Disodium Triphosphate for Bioimaging. *Mater. Sci. Eng., C* **2017**, *76*, 1146-1153.